Mn DOPING OF GaN LAYERS GROWN BY MOVPE

#PETR ŠIMEK, ZDENĚK SOFER, DAVID SEDMIDUBSKÝ, ONDŘEJ JANKOVSKÝ, JIŘÍ HEJTMÁNEK*, MIROSLAV MARYŠKO*, MICHAL VÁCLAVŮ**, MARTIN MIKULICS***

Dept. of Inorganic Chemistry, Institute of Chemical Technology, Technicka 5, 166 28 Prague 6, Czech Republic
**Institute of Physics ASCR, v.v.i., Cukrovarnicka 10, 162 53 Prague, Czech Republic*
***Faculty of Mathematics and Physics, Charles University, Ke Karlovu 3, 121 16 Prague, Czech Republic*
****Peter Grünberg Institute (PGI-9), Forschungszentrum Jülich, D-52425 Jülich, Germany*

#E-mail: simekp@vscht.cz

Submitted February 29, 2012; accepted May 11, 2012

Keywords: Metalorganic vapor phase epitaxy, Nitrides, Magnetic materials, Semiconducting III-V materials

In this contribution we present a growth of $Ga_{1-x}Mn_xN$ layers by MOVPE. Mn doped GaN layers were grown with and without undoped GaN templates on (0001) sapphire substrates in a quartz horizontal reactor. For the deposition of $Ga_{1-x}Mn_xN$ layers $(MCp)_2Mn$ was used as a Mn – precursor. The flow of the Mn precursor was 0.2-3.2 µmol.min^{-1}. The deposition of $Ga_{1-x}Mn_xN$ layers was carried out under the pressure of 200 mbar, the temperature 1050 °C and the V/III ratio of 1360. For the growth of high quality GaN:Mn layers it was necessary to grow these layers on a minimally partially coalesced layer of pure GaN. The direct deposition of GaN:Mn layer on the low temperature GaN buffer layer led to a three-dimensional growth during the whole deposition process. Another investigated parameter was the influence of nitrogen on the layer's properties. A nearly constant ferromagnetic moment persisting up to room temperature was observed on the synthesized thin films.

INTRODUCTION

The present generation of semiconductor electronic and photonic devices is based on transporting a charge of electrons and holes. The field of semiconductor spintronics seeks to exploit the spin of charge carriers in a new generation of transistors and lasers which are going to be employed in ultra-low power high-speed memory and photonic devices. The practical developments of these novel spin-based devices depend on the availability of materials with magnetic ordering temperature (T_C) above room temperature [1]. In the last decade the research of dilute magnetic semiconductors (DMS) was mainly concerned with the transition metal doped gallium arsenide [2]. These narrow band-gap materials exhibit ferromagnetic behavior deep below room temperature. The highest T_C observed for $Ga_xMn_{1-x}As$ has reached about 170 K [2]. Such a low T_C is probably due to a long-distance but weak interaction between Mn atoms being mediated by itinerant charge carriers. For wide band-gap materials doped by transition metals (TM), T_C over room temperature has been predicted [1]. This has been confirmed for $Ga_xMn_{1-x}N$ and $Ga_xCr_{1-x}N$ where $T_C \sim 350$ K has been reported [3, 4]. The usual way to prepare these materials is the MBE technique. Compared to MBE, MOVPE growth of Mn doped nitrides offers large scale production of high quality epitaxial layers for future devices.

In this work we present the growth of Mn doped GaN layers on sapphire substrates and GaN/sapphire templates. GaN template layers were grown at low pressure MOVPE on c-plane sapphire substrates and $Ga_xMn_{1-x}N$ was subsequently deposited. Chemical composition of the layers was measured by WDX and SIMS. Magnetic behavior of the layers was investigated using Quantum Design MPMS and EPR and transport properties by the Hall effect measurement in van der Pauw configuration. Structure characterizations were done by XRD and Raman spectroscopy.

EXPERIMENTAL

GaN templates were grown on c-plane (0001) epi-ready sapphire wafers (10×20 mm) slightly miscut by about 0.2° towards the c-plane in a quartz horizontal reactor. The low temperature GaN buffer layer with a thickness of about 35 nm was applied in all growth experiments. The high temperature template layer was deposited at 1100 °C and the pressure 200 mbar. For the deposition of $Ga_{1-x}Mn_xN$ layers, $(MCp)_2Mn$ was used as a Mn precursor. The flow of Mn precursor was varied in the range 0.2-3.2 µmol·min^{-1}. The $Ga_{1-x}Mn_xN$ layer was deposited under the same conditions in all experiments. The maximal used flow of Mn precursor matches the theoretical concentration of the Mn in the layer of about

3.8 at.%. The total flow of gases was 3700 sccm and the nitrogen concentration in the carrier gas was up to 40 %. As for the pure GaN templates, the deposition was carried out under the pressure of 200 mbar, the temperature 1050 °C and the V/III ratio of 1360. The typical thickness of the $Ga_{1-x}Mn_xN$ film alternated from 35 nm representing the thickness of the low temperature GaN buffer layer up to 1 mm for thick template GaN layer.

Chemical composition of the layers was measured by SIMS and electron microprobe with a wavelength dispersive X-ray detector (WDX) performed on JEOL JXA 733 microanalyzer. These WDX analyses were used for the estimation of the total Mn concentration in the layer. The energy of the electron beam with 0.5 mm diameter was 15 keV. The signal from Mn-K_α line was measured on a wavelength dispersive analyzer and was used for the estimation of Mn concentration. Data obtained by PIXE analysis were used for the exact calibration of WDX and SIMS. The concentration profiles of Mn were determined by SIMS. The SIMS analysis was performed with Perkin Elmer PHI 600 series instrument. A Cs^+ primary ion beam with an energy of 3.0 keV and a flux ~18 nA was focused to a diameter of ~30 mm and raster-scanned across a sample area of 400 x 1000 mm under the incidence angle of 60 degrees (relative to the sample normal). The secondary ion signal was detected by a quadrupole mass analyzer. Sample charging was compensated by the low energy electron bombardment. Surface morphology of the layers was studied by AFM and optical microscopy with DiC. Structure quality of the layers was probed by XRD and Raman spectroscopy with high resolution. The magnetization was measured on MPMS (Quantum Design) in the temperature range of 5 - 330 K. The conventional measurement procedure in a constant magnetic field and under varying temperature could not be employed in this case due to the diamagnetic signal of the substrate being of comparable magnitude to the intrinsic ferromagnetism of the Mn doped layers. Hence, the magnetization was recorded vs. magnetic field varying from 0 to 5 T at a constant temperature and the resulting magnetization curves were corrected by subtracting the diamagnetic addenda of the GaN substrate. The transport properties were characterized by Hall effect measurement in van der Pauw configuration. Raman spectra were measured by Joblin Yvon Labaram HR spectrometer with confocal microscope Olympus. For the excitation the 532 nm Ar laser with 50 mW output power was used. The spectrometer is equipped with the grating 1800 mm^{-1} and CCD camera. Renishav micro-PL setup connected to Leica microscope was used for the photoluminiscence measurement. The 325 nm He-Cd laser with 25 mW output power was used for the excitation. The spectrometer is equipped with the grating 2400 cm^{-1} and high sensitivity CCD camera.

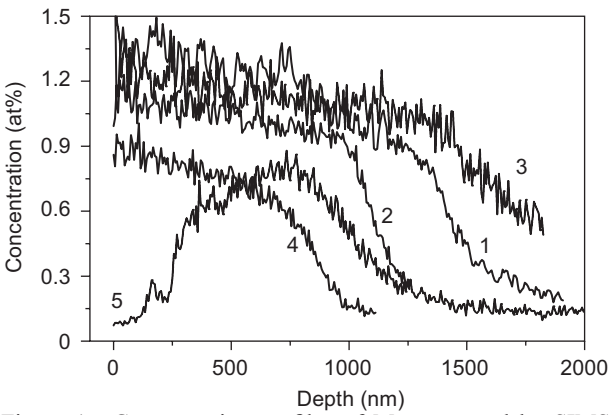

Figure 1. Concentration profiles of Mn measured by SIMS (1 - 1000 nm GaN, 2 - 350 nm GaN, 3 - 520 nm GaN, 4 - 500 nm GaN/40 % N_2, 5 - 50 nm GaN).

RESULTS AND DISCUSSION

The concentration profiles of GaN:Mn layers were measured by SIMS (see Figure 1). The manganese concentration in the layer is almost independent on the thickness of GaN buffer layer with only the exception of the GaN:Mn layer deposited without the high temperature buffer layer. A very peculiar concentration profile is observed in this case. Unlike other samples, the manganese concentration in the layer is not constant, but it exhibits a maximum at about 1500 nm below the surface suggesting the Mn-incorporation is likely more suppressed during the pure three-dimensional growth. The concentration of Mn in the layers deposited with the application of GaN templates was about 1.2 at.%. This value is about 3 times lower then the manganese-gallium rate in the gas phase. In other experiments we used hydrogen-nitrogen carrier gas mixture. We observed a strong suppression of Mn concentration in the layer with the increasing nitrogen concentration in the carrier gas. The average concentration of Mn in the $Ga_{1-x}Mn_xN$ layer deposited with 40 % of nitrogen in the carrier gas decreased down to 0.8 at.%. This can be explained by slower diffusion of Mn precursor in the carrier gas with nitrogen. The influence of nitrogen activity in the atmosphere on the solubility of Mn in GaN is another important factor. As it has been demonstrated by thermodynamic calculations [9], the higher nitrogen partial pressure causes the suppression of Mn equilibrium concentration in GaN.

The thickness of the GaN buffer layers has a notable influence on the surface morphology of the subsequently deposited Mn doped GaN layers. We investigated the influence of GaN buffer layer thickness on the structural, electrical and magnetic properties of the layer. A decrease of pure GaN layer thickness led to a significant deterioration of surface morphology of the deposited GaN layer. It was necessary to grow GaN:Mn layers on at least partially coalesced layer of pure GaN to obtain good surface morphology with low

root mean square (RMS) roughness. A direct deposition of GaN:Mn layer on low temperature GaN buffer layer led to the pure three-dimensional growth during the whole deposition process. This effect subsequently strongly influences the manganese incorporation into the growing layer. Rectangular blocks of the size below 1 mm were observed on the layer surface. Decreasing the buffer layer thickness led to the creation of vertical steps between these "blocks". One hour growth didn't lead to the change of the growth mechanism to two dimensional. mode. The surface morphology obtained by AFM is shown in Figure 2. The development of the surface morphology with buffer layer thickness is demonstrated on Figure 3.

The rocking curves of (002) reflection reveals an opposite behavior, i.e. the suppression of buffer layer thickness led to a substantial improvement of the layer structure quality (FWHM decreased from 669 to 366 arcsec.). This observation indicates that "blocks" on the layer surface are strongly related to the structure quality of the layer and coalescence of the layer induces a biaxial strain and a formation of screw and mixed type dislocations. Strain relaxation of the layer observed by Raman spectroscopy has significant effect on the reduction of dislocation density. A decrease of FWHM for (002) rocking curve indicates that the concentration of screw and mixed type dislocations is diminished. The implementation of Mn at the beginning of the layer growth can also induce a suppression of screw type dislocation concentration. The dependence of FWHM for (002) reflection is shown in Figure 3. The application of nitrogen as a carrier gas also plays an important role in the development of the layer morphology [10], which turned out to be considerably improved. On the other hand, this improvement is accompanied by an increase of biaxial strain and dislocation density in the layer. The growth rate and time of coalescence decreased in this case.

The influence of Mn doping on the structure properties was investigated by Raman spectroscopy. The measured Raman spectra are plotted in Figure 4. We observed a substantial release of biaxial strain represented by the shift of E_2 (high) vibration mode from 568.6 cm^{-1} to 567.8 cm^{-1} for the GaN:Mn layer with 1 mm thick GaN buffer layer and the GaN:Mn layer without any buffer layer, respectively. The latter value is almost identical as for the strain free bulk GaN (567.7 cm^{-1}). The application of Mn led to an extreme decrease of the layer strain. These results can be attributed to an incomplete coalescence of the layers without GaN buffer layer. The layers deposited with an addition of nitrogen in the carrier gas exhibited an extremely high biaxial strain (569.6 cm^{-1}), which is responsible for the cracks observed on the layer surface. The vibration band centered at 669 cm^{-1} is mainly related to the manganese incorporation into the layer. Simultaneously, this vibration mode is associated with local vibration modes (LVM) introduced by nitrogen vacancies [7]. The nitrogen vacancies are probably generated in order to compensate Mn in the interstitial positions in the GaN host lattice.

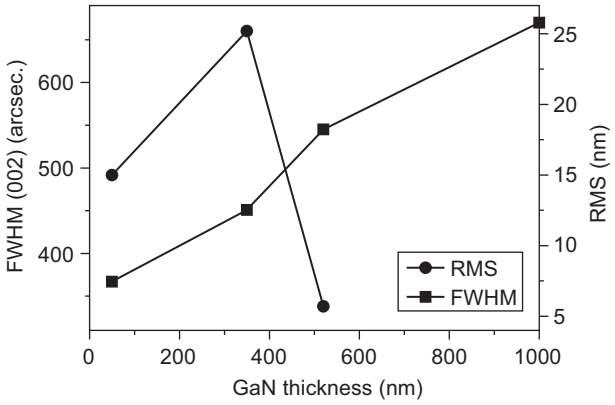

Figure 3. The dependence of surface roughness (RMS) and FWHM of (002) reflection on the buffer layer thickness.

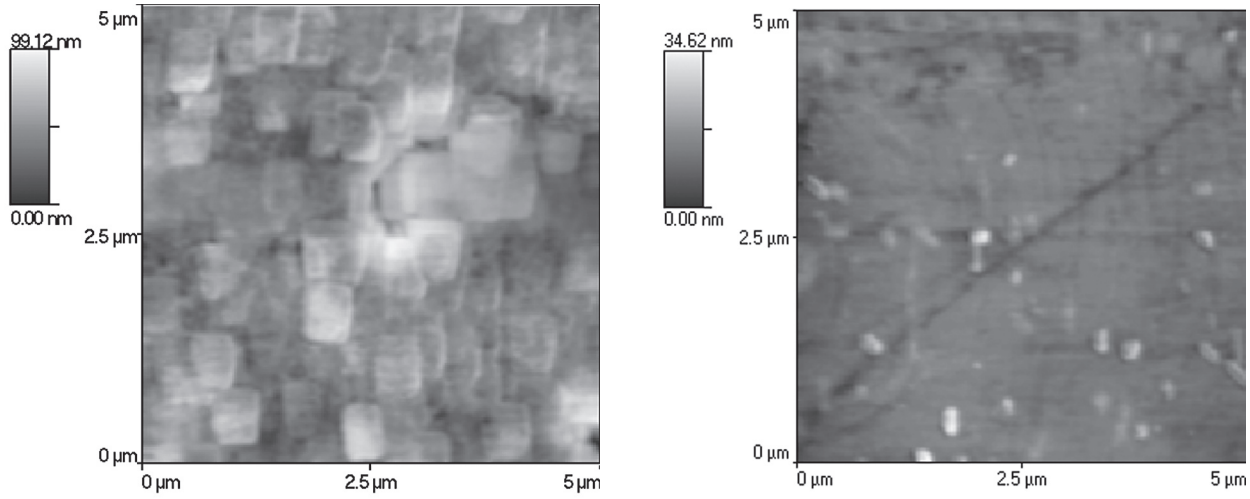

Figure 2. The surface morphology of the layer grown without high temperature GaN buffer layer (left) and with 1 µm thick GaN buffer layer (right).

The intensity of LVM vibration mode scales the total amount of manganese in the layer. The vibration mode related to Mn → Ga substitution is visible at 575-580 cm^{-1}. This is an indication of partial gallium substitution by manganese in wurtzite structure. Other Raman vibration modes were observed at 735 cm^{-1}, 560 cm^{-1} and 533 cm^{-1} respectively, corresponding to A_1(LO), E_1(TO) and A_1(TO) symmetries [5]. We observed an intensity enhancement of A_1(LO) vibration mode with increasing thickness of the Mn-doped layer. Correspondingly, the suppression of free carrier concentration is apparent due to the large binding energy of Mn acceptors acting as deep lying trapping centers for doped electrons [6]. These results are in a good agreement with free carrier concentration measurements. These data predominantly reflect the transport characteristics of the pure GaN template layer. However, the sample grown without the template layer exhibited high concentration of free carriers. This can be explained by high concentration of defects in the layer. A decrease of buffer layer thickness was accompanied by a strong decrease of free carrier mobility from 49.4 $cm^2\ V^{-1}\ s^{-1}$ for the layer with 1 mm thick GaN buffer layer down to 19.9 $cm^2\ V^{-1}s^{-1}$ for the layer without GaN buffer layer.

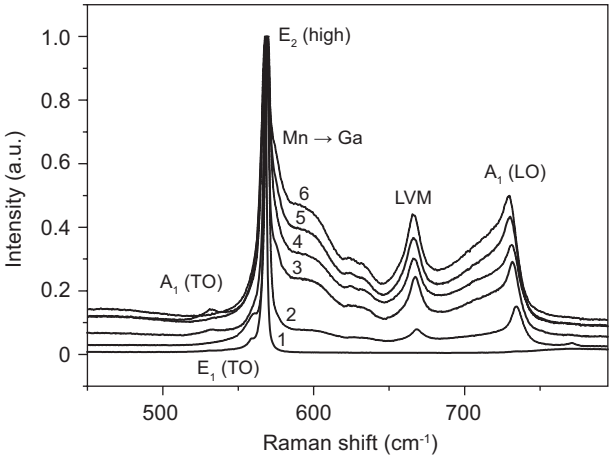

Figure 4. Raman spectra of GaN:Mn layers (1 - FS GaN, 2 - 50 nm GaN, 3 - 1000 nm GaN, 4 - 500 nm GaN/40 % N_2, 5 - 520 nm GaN, 6 - 350 nm GaN).

Figure 5 shows the PL emission spectra of Mn doped layers and pure GaN layer measured at 300 K. The peak emission energy for the as-grown layers is located at the energy of 3.43 eV. Free excitons, with the low binding energy at room temperature, are thermally dissociated and the spectrum is determined by free to free and free to bound transitions. This is the origin of spectrum broadening. The sample with 50 nm pure GaN layer has a maximum shifted by about 10 meV to higher energy which could be attributed to huge density of threading dislocations as a result of three dimensional growth. Huge concentration of dislocations is also responsible for the much wider band. The lower wing of the PL spectra is due to transitions from the density of states tail. The phonon replicas were observed in Mn-doped samples at 3.47 eV and 3.52 eV. Additional peak is observed at 3.36 eV which could be attributed to the shallow donors caused by defects and impurities.

According to Coey et al. [8], the magnetic impurities can form bound magnetic polarons with charge carriers occupying the donor levels associated with non-magnetic dopants such as nitrogen vacancies or other electron donors (like oxygen). In our case, the charge neutrality condition suggests a formation of large number of these defect. However, these do not bring any additional electrons as they just compensate for Mn^{2+} and are likely to bound to them. Hence, only the native donor levels occupied by extra electrons can be involved in such magnetic polarons. The probability of their population is indeed highly reduced as the concentration of magnetic dopants acting as trapping centers increases.

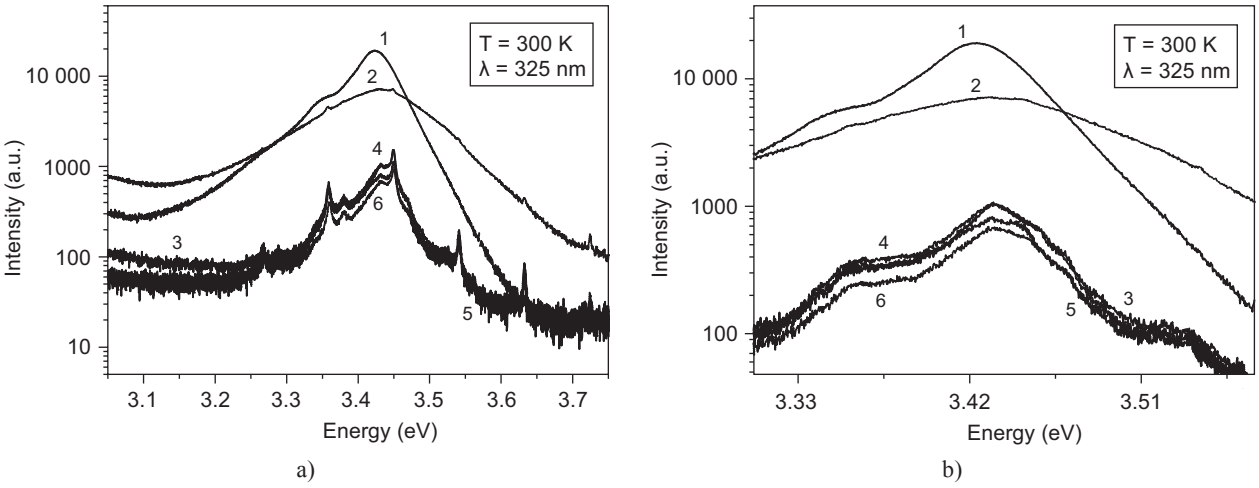

Figure 5. Photoluminescence of GaN:Mn layers (1 - undoped GaN, 2 - 50 nm GaN, 3 - 1000 nm GaN, 4 - 500 nm GaN/40 % N_2, 5 - 520 nm GaN, 6 - 350 nm GaN).

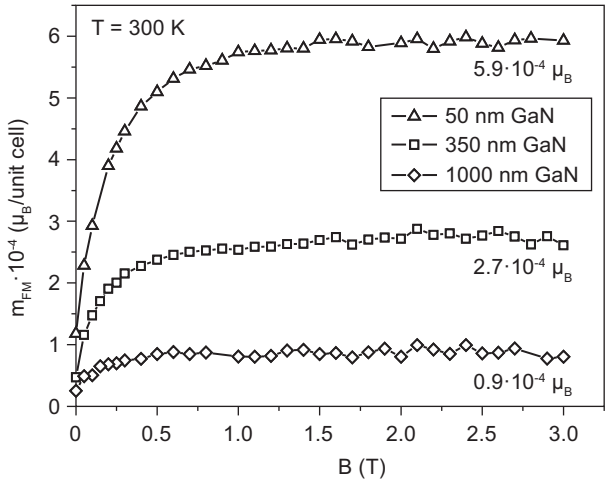

Figure 6. Ferromagnetic moment of GaN:Mn layers.

The occurrence of ferromagnetism (Figure 6) thus seems to be confined to a highly dilute regime (less than 1 at.% Mn) far below the value of ~ 5 at.% Mn which had been originally considered as optimum for the establishment of FM state. Unfortunately, since it is also far below the percolation limit for itinerant ferromagnetism, the concomitance with a PM phase can be hardly avoided.

CONCLUSIONS

We studied the influence of the buffer layer thickness and carrier gas composition on the properties of the Mn doped GaN layer. The thickness of the GaN buffer layer has a considerable influence on the structural properties of the layer and on the growth process. A decrease of buffer layer thickness led to a suppression of 2D mode growth which was accompanied by the destruction of the surface morphology and by a decrease of biaxial strain and dislocation density. This subsequently affected the incorporation of Mn into the growing layer. The influence of nitrogen in the carrier gas was also appreciable and led to a fast coalescence with good surface morphology of the layer and high biaxial strain. A strong decrease of carrier mobility was also observed with decreasing GaN buffer layer thickness. Layers exhibit ferromagnetic behavior persisting up to 300 K.

Acknowledgements

This work was supported by the Czech Science Foundation (project N° 104/09/0621 and 106/09/0125) and Ministry of Education of the Czech Republic (research projects N° MSM6046137302). Financial support from specific university research (MSMT No 21/2012).

References

1. Dietl T.: Phys. Status Solidi B *240*, 433 (2003).
2. Jungwirth T., Niu Q., MacDonald A.H.: Phys. Rev. Lett. *88*, 207208 (2002) .
3. Cho Y.S., Kaluza N., Guzenko V., Schäpers T., Hardtdegen H., Bochem H.-P., Breuer U., Ghadimi M.R., Fecioru-Morariu M., Beschoten B., Lüth H.: Phys. Status Solidi A *204,* 2729 (2007).
4. Chena Z.T., Sua Y.Y., Yanga Z.J., Zhang B., Xu K., Yang X.L., Pan Y.B., Zhang G.Y.: J. Cryst. Growth *298,* 254 (2007).
5. Fenwick W.E., Asghar A., Gupta S., Kang H., Strassburg M., Dietz N., Graham S., Kane M.H., Ferguson I.T.: J. Vac. Sci. Technol. A *24,* 1640 (2006).
6. Limmer W., Ritter W., Sauer R., Mensching B., Liu C., Rauschenbach B.: Appl. Phys. Lett. *72,* 2589 (1998).
7. Gebicki W., Strzeszewski J., Kamler G., Szyszko T., Podsiadło S.: Appl. Phys. Lett. *76,* 3870 (2000).
8. Coey J.M.D., Venkatesan M., Fitzgerald C.B.: Nature Materials *4,* 173 (2005).
9. Sedmidubský D., Leitner J., Sofer Z.: J. Alloy. Compd. *452,* 105 (2008).
10. Cho Y.S., Hardtdegen H., Kaluza N., Thillosen N., Steins R., Sofer Z., Lüth H.: Phys. Status Solidi C *3,* 1408 (2006).